Understanding of the Retarded Oxidation Effects in Silicon Nanostructures

Christophe Krzeminski, Xiang-Lei Han, Guilhem Larrieu

Understanding of the Retarded Oxidation Effects in Silicon Nanostructures

C. Krzeminski,[*,†] X.-L. Han,[†] and G. Larrieu[*,‡]

IEMN-UMR CNRS 8520, Département ISEN, Avenue poincaré, 59650 Villeneuve d'Ascq, France, and LAAS/CNRS, Université de Toulouse, 7, av. du Colonel Roche 31077 Toulouse Cedex 4, France

E-mail: christophe.krzeminski@isen.fr; guilhem.larrieu@laas.fr

Abstract

A new understanding of the retarded or self-limited oxidation phenomenon observed during the oxidation of silicon nanostructures is proposed. The wet thermal oxidation of various silicon nanostructures such as nanobeams, concave/convex nanorings and nanowires exhibits an extremely different and complex behaviour. Such effects have been investigated by the modelling of the mechanical stress generated during the oxidation process explaining the retarded or quasi self-limited regime. The proposed model describes the oxidation kinetics of silicon nanowires down to a few nanometers while predicting reasonable and physical stress levels at the Si/SiO_2 interface by correctly taking into account the relaxation effects in silicon oxide through plastic flow. Finally, this study gives more insight into the retarded or self-limiting oxidation phenomenon.

[*]To whom correspondence should be addressed
[†]IEMN-UMR CNRS 8520, Département ISEN, Avenue poincaré, 59650 Villeneuve d'Ascq, France
[‡]LAAS/CNRS, Université de Toulouse, 7, av. du Colonel Roche 31077 Toulouse Cedex 4, France

Stress engineering has been successfully introduced by the semiconductor industry to enhance the channel device mobility.[1] A similar approach, where a stress field is introduced during the fabrication process, could be considered as an interesting tool to achieve an optimal control of the nanoobject fabrication. Silicon oxidation, where the tuning of process parameters for the stress development is known[2] but not really understood at the nanoscale level, is the most striking example. Retarded oxidation where the oxide growth slows down very rapidly with oxidation duration or with the silicon nanoobject dimension is still a puzzling physical effect. For a dry oxidation and a low thermal budget, a short initial regime where the oxidation rate decreases very quickly is observed. The oxidation of small silicon nanoobjects such as small nanoislands,[3] nanospheres,[4] nanoclusters[5] or nanowires[6,7] is known to be significantly retarded compared to planar oxidation rate performed with the same experimental conditions. This retardation effect is observed to be more pronounced with decreasing curvature radius for Si nanowires[7,8] or triangle-shaped nanostructures.[9] Self-limited effects follow the retarded regime where the oxidation reaction completely stops at the atomic level and no further oxide is created despite an exposure to the oxidising ambient during several hours.[6] With the silicon core resulting from these self-limited effects, the fabrication of silicon pillars in the 2-16 nm range[6,7] and horizontal nanowires down to 8 nm[10] with a control less than 1 nm have been demonstrated. This physical effect can be viewed as a technological nanoscale tool able to control the nanoobjects shape,[11] size distribution[12] interface properties[13] and could be implemented in many applications like : sub-5 nm transistor,[14] light emission[15] or nanoflash memory.[16,17] However, only very few experimental studies have been dedicated to the understanding of the phenomenon which remains fragmented and limited.[6,18,19] In this work, oxidation kinetics have been investigated both on the experimental and theoretical counterparts in order to improve the understanding of the mechanisms of retarded and self-limited mechanisms and to quantify the amount of stress generated at the Si/SiO_2 interface in silicon nanostructures.

Generally self-limited oxidations are performed experimentally in dry ambient at low temperature with many hours of oxidation. Wet oxidation is characterised by a larger reaction rate but a lower ambient diffusivity[20] compared to dry oxidation and should be of particular interest to elucidate the self-limited mechanism. With the nowdays top-down fabrication capabilities,

etched silicon nanostructures including nanobeams, nanorings and nanowires have been fabricated with a high resolution as shown in Figure 1 (fabrication details are given in supplementary information) and next oxidized at 850°C. The seminal work of Kao *et al.*[21,22] with micrometer size of 2D cylindric object has been revisited but in the nanometric range. Experimentally, the oxidation kinetics have been observed to be strongly dependent on the size and the geometry of the nanoobject. Figure 2.a) summarises the evolution of the oxide thickness as a function of the oxidation duration in the case of convex (SiNWs) and concave (Si nanorings) structures. The oxide growth rate is strongly limited with the oxidation time but is faster in a convex structure than in a concave one. The influence of the geometrical effect is stronger with smaller inner radius (i.e. 70 nm compared to 430 nm). For the convex case, a higher oxide growth rate is related to the larger radii. Then, in order to investigate experimentally the influence of silicon nanostructure dimension, nanobeams and nanowires of height 240 nm have been oxidized for 10 and 20 minutes. As shown in Figure 2.b).(1), a non-uniform oxide growth is classically observed along the sidewall of the beam due to the great influence of the top and bottom corners corresponding to a convex and concave structure respectively. Oxidized one-dimensional nanostructure with diameters from 40 nm to 140 nm demonstrated completely different shapes as shown in Figure 2.b).(2) with the presence of a pinching effect at the bottom of Si nanobeam structures. In order to compare the oxidation between the two structures, the oxide thicknesses have been measured in the middle of these vertical structures described in SEM images and are plotted in the Figure 2.b). The oxide growth on Si nanobeams of previous width L is clearly thicker than a SiNWs with the diameter $d = L$. A size dependent oxidation kinetic was not observed in these structures whatever the nanobeam width considered. These experimental results illustrate that the silicon oxidation retarded mechanism is strongly dependent at the nanoscale level on the nanoobject i) dimension ii) size and iii) shape as function of the concav/convex surface character.

These dependence cannot be explained by the standard Deal and Grove oxidation model[20] as for example a larger oxidant concentration for the smallest particles should in principle lead to a higher oxidation rate. Two main theories have been put forward to explain the self-limiting kinetics factor. The first one is the "stress limited reaction rate" assumption.[19] In this case,

the radial stress build-up at the Si/SiO_2 interface is assumed to be linearly dependent of the oxidation time up to a critical stress estimated to a few GPa where the oxidation rate would be completely negligible. First principle simulations tend to support the conclusion that the energy barrier reaction increases with the stress present at the Si/SiO_2.[23] The second theory is the "diffusion limited mechanism" where a significant increase in the activation energy of the oxidant diffusivity in the highly stressed region is advanced[6] and a new oxidation kinetic model based on the variation of the diffusion activation along the SiNWs radius is proposed.[24] This point is also supported by atomistic simulations where a density increase (2.7 g/cm^2) is predicted by molecular dynamic simulations.[25] According to first principle calculations,[26] compressively strained silicon oxides exhibit larger activation barrier for the diffusion and volume incorporation of oxygen species. In this framework, the origin of self-limited effects would be the oxidant species supply at the Si/SiO_2 interface which is limited by the stress influence on the oxidant diffusion and incorporation. Despite the fact that an unknown and uncontrolled amount of strain is introduced during the reaction, no quantitative determination of the mechanical stress build-up during processing is provided by the two approaches.

In order to model the oxidation of the nanoobjects with cylinder geometry, the extended Deal and Grove model[22] in cylindrical coordinates has been used.[22] The wet oxidation rate v at the Si/SiO_2 interface is given by Eq. (1):

$$v = \frac{(\alpha - 1)C^*}{N} \cdot \frac{1}{\frac{1}{k_{Si}^{\sigma}} \pm \frac{a}{D^p} \log\left(\frac{b}{a}\right)} \tag{1}$$

with respectively a (b) the inner (outside) radius, α the volume expansion factor of silicon to oxide conversion (2.25), N the number of oxidant molecules incorporated into a unit volume of silicon oxide, the $+$ (resp. -) sign denotes the convex (concave) surface. This equation classically takes into account that the surface curvature influences the oxidant concentration and in the convex (concave) configuration, the concentration increases (decreases). In our approach, both the reaction rate k_{Si}^{σ} at the Si/SiO_2 interface and the diffusivity in the silicon oxide D_{SiO_2} are stress dependent. These dependences are taken into account and the oxidation is either limited by the reaction rate or/and by the oxidant supply through the reduced oxidation

diffusion. The dominant mechanism which strongly depends on the nanoobject geometry will be discussed later.

The reaction rate k_{Si}^{σ} is directly proportional to the linear rate constant $(B/A)_{[110]}(T)$ ((5.18 10^{-09} nm/s at 850°C)) defined in the Deal and Grove approach by introducing C^* the oxidant solubility in the silicon dioxide and is strongly dependent on the radial stress component σ_r at the Si/SiO_2 interface :

$$k_{Si}^{\sigma} = \frac{N}{C^*} \cdot (B/A)_{[110]}(T) \exp\left(\frac{\sigma_r V_k}{k_B T}\right) \tag{2}$$

where k_B is the Boltzmann constant, T is the oxidation temperature and V_k (15 Å^3) corresponds to the activation volume. A compressive radial stress ($\sigma_r < 0$) slows down the linear rate oxidation rate. The term $(B/A)_{[110]}(T)$ takes into account the influence of the $[110]$ crystalline orientation and the factor taking into account orientation effects has been calibrated with planar bulk oxidation experiments [1]. Next the oxidant diffusivity, D_{SiO_2} :

$$D_{SiO_2} = \frac{N}{2C^*} \cdot B(T) = \frac{N}{2C^*} \cdot B_0(T) \cdot \exp\left(\frac{-PV_d}{k_B T}\right) \tag{3}$$

is linearly dependent on the initial parabolic constant $B_0(T)$ (2.68 10^{-13} nm^2/s at 850°C) and is limited by a compressive ($P > 0$) hydrostatic pressure $P = -0.5 \cdot (\sigma_r + \sigma_\theta)$ in the silicon oxide (V_d=45 Å^3). A tensile pressure increases the diffusivity up to an arbitrary limit fixed at 20%. These assumptions are often estimated to be equivalent to a diffusivity dependence with oxide density.[27]

A major issue in oxidation modelling is a proper description of the mechanical behaviour of silicon dioxide as shown in Figure 3 and its ability to store or to dissipate mechanical energy. A shortcoming is observed for the viscous approach[22,28] for our experimental conditions (low temperate, large initial deformation rate) since the compressive radial stress at the interface is inversely proportional to the curvature radius of the nanoobject. In the case of cylinder oxidation, it has been shown that a viscous mechanical behaviour considered in the work of Kao et

[1] A particular attention has been paid to measure the oxidation thickness along this orientation for the different nano-objects

al.[22] strongly overestimates the stress level[29] and could reach an unphysical value. Atomistic simulations and in particular, molecular dynamics simulation results on limited silicon oxidation[25,30,31] should also be considered with high care as a poor description of the stress field in the case of compressive strained SiO_2 structures is given and stress levels predicted are often overestimated by one order of magnitude.[32] The main reason is that the irreversible atomic rearrangements occuring with large shearing forces[33] are neglected. Such localised flows of defects introduced in a relatively rigid amorphous structure increase the material fluidity. This plastic flow has been described by a shear dependent viscosity[34] :

$$\eta(\tau) = \eta_0(T)\frac{\tau/\sigma_c}{\sinh(\tau/\sigma_c)} \tag{4}$$

where $\eta_0(T)$(is the low stress viscosity, τ the shear stress and σ_c is the critical stress threshold where plasticity flow should appear (1 GPa). The low stress viscosity value (1.4 10^{18} Poisse at 850°C) considered is characteristic of a wet oxide with a high viscosity induced by the presence of hydroxyl content.[35] In this physical picture, the mechanical behaviour of the silicon oxide, upon reaction and under large forces, is strongly influenced by the shear stress τ which is more fluid and decreases the silicon oxide viscosity η. In reaction, the various stress components are reduced whereas in the same time the oxide growth rate v at the interface is slowed down. Several works[27,36] have also considered a shear dependent viscosity in order to introduce plasticity effects. It could be noticed by the expression of the shear stress :

$$\tau(r) = \frac{2\eta a v}{r^2} \tag{5}$$

that the oxidation growth rate Eq. (1), the shear dependent viscosity Eq. (2) and finally the shear stress Eq. (5) are coupled with each others. The fact that all of these equations must be *self-consistently* solved is often overlooked or not exactly taken into account. Following Rafferty *et al.*,[37] the shear (τ), radial (σ_r) and tangential (σ_θ) stress field component in the silicon dioxide of a cylinder structure (see Figure 1.b) can be expressed as :

$$\begin{cases} \tau(r) = \sigma_c \sinh^{-1}\left(\dfrac{2R^2}{r^2}\right) \\ \sigma_r(r) = \pm\frac{1}{2}\sigma_c\left[\left(\ln\dfrac{R^2}{b^2}\right)^2 - \left(\ln\dfrac{R^2}{r^2}\right)^2\right] \\ \sigma_\theta(r) = \sigma_r(r) - 2\tau(r) \end{cases} \quad (6)$$

with the reduced parameter $R = \sqrt{\frac{4\eta_0 a v}{\sigma_c}}$. Compared to a standard viscous approach[22] with a constant viscosity, the radial stress build-up has a logarithmic dependence on the curvature radius which gives us the opportunity to investigate the oxidation of cylinder shape nanostructures.

The retarded and self-limited experimental oxidation effect have been investigated using this plastic model. Figure 4.a) shows that the influence of concave or convex character on the retarded oxidation effects can be well predicted by the model. As shown in Figure 4.b) a substantial non-linear increase is observed for the compressive radial stress component at the Si/SiO_2 interface up to a few GPa, coupled with an initial tensile hydrostatic pressure (inset Figure 4.b). These elements clearly indicate that a reaction limited process takes place in the convex configuration. The situation is totally different in the concave case where a radial compressive stress build-up remains limited but the compressive hydrostatic pressure clearly impacts the oxidant diffusivity. In that case, the major limiting factor is the diffusion mechanism which reduces the oxidant supply. A quasi self-limited oxidation for 70 nm concave structure is observed and can be correlated to the occurrence of both a diffusion and reaction limited regime. As summarized by Table 1, the dominant retardation mechanism is strongly dependent on the surface shape but can be explained by the variation of the stress field component at the Si/SiO_2 in agreement with previous results.[22]

Next, Figure 5.a) compares the experimental SiNW oxidation kinetics (symbols) for various SiNW diameters and the modelling. These experimental data are also nicely described by the plastic oxidation modelling. While being close to the linear bulk oxidation kinetics in the short time regime, the kinetics reveal a retarded and diameter dependent regime with a quasi self-limited oxidation effects for the thinnest SiNWs. Figure 5.b) gives the prediction of stress field evolution during the reaction. Large non-linear build-up as a function of the oxidation time for

the compressive radial stress down to 3 GPa have been obtained but remains compatible with the interfacial stress estimated in VLS-grown SiNWs using contact-resonance atomic force microscopy.[38] This result clearly demonstrates that the radial stress build-up is not linear with time as assumed in a previous study.[19] In the same time, a large relaxation for the tangential stress is reported from several GPa down to only few MPa (shown in inset of Figure 5.b) while the compressive shear stress remains nearly constant above the critical stress value of $\sim$ 1GPa assumed in Eq. (4) (see supporting information). Such similar behaviours for the shear stress have been observed in the viscoelastic simulation of the silicon micrometer range cylinder.[36] These simulations explain well the difference in term of behavior between the nanobeams and the nanowires since FEM simulations estimate a much lower compressive stress build-up in the nanobeam.

Finally, the physical origin of retarded oxidation effects observed in SiNWs as a function of the diameter is discussed. Figure 6.a) shows the linear rate variation for the corresponding experimental range. A strong decrease in the reaction rate with radial stress build-up as a function of SiNW diameters is predicted which could be directly correlated to the large radial stress build up depicted in Figure 6.c). This effect cause the initial retarded effects observed in the oxidation of convex nanostructures. On the other hand, Figure 6.b) presents the evolution of the parabolic rate with NW diameters. A decrease in the parabolic rate is observed after a significant delay which can be correlated to the tangential stress relaxation as shown in Figure 6.c). This diffusion limited effect generated by a compressive hydrostatic pressure is probably very much difficult to control from the technological point of view as a time and diameter dependence is observed in Figure 5.b). The quasi-self limited regime observed in wet oxidation for the thinnest nanowire (40 nm) could be explained by the coexistence of a reaction and diffusion limited mechanism. Figure 6.d) illustrates the plastic relaxation effect as a considerable reduction of the initial silicon dioxide viscosity is predicted ($\eta(\tau)/\eta_0 \ll 1$) reducing the shear stress through Eq. (5) which remains above the critical plastic limits of 1 GPa (see supporting information). For the first time, a reasonable physical picture is provided with a stress build-up in SiNWs at the Si/SiO_2 interface. Moreover the stress magnitude responsible for the retarded or quasi-limited effects are also compatible with the absence of mechanical defects character-

istics[39] of huge mechanical stress (up to several GPa) exceeding the plastic limits of silicon nanowires.

In conclusion, retarded and quasi-limited oxidation kinetics have been investigated at the nanoscale level for different silicon nanoobjects. We have demonstrated experimentally the influence of the nanoobject dimension, size and shape on the oxidation behavior. All of these effects have been correlated to the interfacial stress build-up at the interface Si/SiO_2. For the silicon nanowires, given the deformation rate level under study, modelling aspects show that the mechanical energy dissipation in silicon dioxide through plastic relaxation remains paramount in order to estimate (i) a physical mechanical stress build-up at the interface and (ii) the interface velocity. In order to take into account the stress at the Si/SiO_2 interface responsible for the limited and/or the retarded oxidation effects, both reaction or diffusion limited mechanisms depending on the many experimental conditions. Low temperature wet oxidation, where the reaction could be controlled by the compressive radial stress but not totally limited thanks to the plastic relaxation, is an interesting stress engineering tool. First, with more physical understanding, stress driven processing could be achieved for an optimal control of the SiNWs shape[40] and next as an intentional stress source for SiNWs mobility engineering.[41,42]

Acknowledgement

This work was partially supported by the European Commission through the NANOSIL Network of Excellence (FP7-IST-216171).

References

(1) Mohta, N.; Thompson, S. *IEEE Circuits and Devices Magazine* **2005**, *21*, 18.

(2) Hu, S. M. *Journal of Applied Physics* **1988**, *64*, 323–330.

(3) Okada, R.; Iijima, S. *Applied Physics Letters* **1991**, *58*, 1662–1663.

(4) Hofmeister, H.; Huisken, F.; Kohn, B. *The European Physical Journal D - Atomic, Molecular, Optical and Plasma Physics* **1999**, *9*, 137–140.

(5) Coffin, H.; Bonafos, C.; Schamm, S.; Cherkashin, N.; Assayag, G. B.; Claverie, A.; Respaud, M.; Dimitrakis, P.; Normand, P. *Journal of Applied Physics* **2006**, *99*, 044302.

(6) Liu, H. I.; Biegelsen, D. K.; Ponce, F. A.; Johnson, N. M.; Pease, R. F. W. *Applied Physics Letters* **1994**, *64*, 1383–1385.

(7) Liu, H. I.; Biegelsen, D. K.; Johnson, N. M.; Ponce, F. A.; Pease, R. F. W. Self-limiting oxidation of Si nanowires. *Proceedings of the 16th international symposium on electron, ion, and photon beams*, 1993; pp 2532–2537.

(8) Büttner, C. C.; Zacharias, M. *Applied Physics Letters* **2006**, *89*, 263106.

(9) Liu, J. L.; Shi, Y.; Wang, F.; Lu, Y.; Gu, S. L.; Zhang, R.; Zheng, Y. D. *Applied Physics Letters* **1996**, *69*, 1761–1763.

(10) Kedzierski, J.; Bokor, J.; Kisielowski, C. Fabrication of planar silicon nanowires on silicon-on-insulator using stress limited oxidation. *Papers from the 41st international conference on electron, ion, and photon beam technology and nanofabrication*, 1997; pp 2825–2828.

(11) Single, C.; Zhou, F.; Heidemeyer, H.; Prins, F. E.; Kern, D. P.; Plies, E. Oxidation properties of silicon dots on silicon oxide investigated using energy filtering transmission electron microscopy. *Papers from the 42nd international conference on electron, ion, and photon beam technology and nanofabrication*, 1998; pp 3938–3942.

(12) Coffin, H.; Bonafos, C.; Schamm, S.; Cherkashin, N.; Assayag, G. B.; Claverie, A.; Respaud, M.; Dimitrakis, P.; Normand, P. *Journal of Applied Physics* **2006**, *99*, 044302.

(13) Shiraishi, K.; Nagase, M.; Horiguchi, S.; Kageshima, H.; Uematsu, M.; Takahashi, Y.; Murase, K. *Physica E: Low-dimensional Systems and Nanostructures* **2000**, *7*, 337 – 341.

(14) Walavalkar, S. S.; Hofmann, C. E.; Homyk, A. P.; Henry, M. D.; Atwater, H. A.; Scherer, A. *Nano Letters* **2010**, *10*, 4423–4428.

(15) Trivedi, K.; Yuk, H.; Floresca, H. C.; Kim, M. J.; Hu, W. *Nano Letters* **2011**, *11*, 1412–1417.

(16) Tang, X.; Reckinger, N.; Bayot, V.; Krzeminski, C.; Dubois, E.; Villaret, A.; Bensahel, D.-C. *Nanotechnology, IEEE Transactions on* **2006**, *5*, 649 –656.

(17) Tang, X.; Krzeminski, C.; Lecavelier des Etangs-Levallois, A.; Chen, Z.; Dubois, E.; Kasper, E.; Karmous, A.; Reckinger, N.; Flandre, D.; Francis, L. A.; Colinge, J.-P.; Raskin, J.-P. *Nano Letters* **0**, *0*, null.

(18) Shir, D.; Liu, B. Z.; Mohammad, A. M.; Lew, K. K.; Mohney, S. E. *Journal of Vacuum Science & Technology B: Microelectronics and Nanometer Structures* **2006**, *24*, 1333–1336.

(19) Heidemeyer, H.; Single, C.; Zhou, F.; Prins, F. E.; Kern, D. P.; Plies, E. *Journal of Applied Physics* **2000**, *87*, 4580–4585.

(20) Deal, B. E.; Grove, A. S. *Journal of Applied Physics* **1965**, *36*, 3770–3778.

(21) Kao, D.-B.; McVittie, J.; Nix, W.; Saraswat, K. *Electron Devices, IEEE Transactions on* **1987**, *34*, 1008 – 1017.

(22) Kao, D.-B.; McVittie, J.; Nix, W.; Saraswat, K. *Electron Devices, IEEE Transactions on* **1988**, *35*, 25 –37.

(23) Akiyama, T.; Kageshima, H.; Uematsu, M.; Ito, T. *Japanese Journal of Applied Physics* **2008**, *47*, 7089–7093.

(24) Cui, H.; Wang, C. X.; Yang, G. W. *Nano Letters* **2008**, *8*, 2731–2737, PMID: 18680350.

(25) Ohta, H.; Watanabe, T.; Ohdomari, I. *Japanese Journal of Applied Physics* **2007**, *46*, 3277–3282.

(26) Akiyama, T.; Kawamoto, K.; Kageshima, H.; Uematsu, M.; Nakamura, K.; Ito, T. *Thin Solid Films* **2006**, *508*, 311 – 314, Proceedings of the Fourth International Conference on Silicon Epitaxy and Heterostructures (ICSI-4) - ICSI-4.

(27) Sutardja, P.; Oldham, W. *Electron Devices, IEEE Transactions on* **1989**, *36*, 2415 – 2421.

(28) Fazzini, P.-F.; Bonafos, C.; Claverie, A.; Hubert, A.; Ernst, T.; Respaud, M. **2011**, *110*, 033524.

(29) Rafferty, C. S.; Borucki, L.; Dutton, R. W. *Applied Physics Letters* **1989**, *54*, 1516.

(30) Torre, J. D.; Bocquet, J.-L.; Limoge, Y.; Crocombette, J.-P.; Adam, E.; Martin, G.; Baron, T.; Rivallin, P.; Mur, P. *Journal of Applied Physics* **2002**, *92*, 1084–1094.

(31) Kim, B.-H.; Pamungkas, M. A.; Park, M.; Kim, G.; Lee, K.-R.; Chung, Y.-C. *Applied Physics Letters* **2011**, *99*, 143115.

(32) Watanabe, T. *Journal of Computational Electronics* **2011**, *10*, 2–20.

(33) Falk, M. L.; Langer, J. S. *Annual Reviews* **2011**, *2*, 353 – 373.

(34) Eyring, H. *The Journal of Chemical Physics* **1936**, *4*, 283–291.

(35) Hetherington, G.; Jack, K. H.; Kennedy, J. C. *Physics and Chemistry of Glasses* **1964**, *5*, 130.

(36) Senez, V.; Collard, D.; Baccus, B.; Lebailly, J. *Journal of Applied Physics* **1994**, *43*, 720.

(37) Rafferty, C. S.; Dutton, R. W. *Applied Physics Letters* **1989**, *54*, 1815.

(38) Stan, G.; Krylyuk, S.; Davydov, A. V.; Cook, R. F. *Nano Letters* **2010**, *10*, 2031–2037, PMID: 20433162.

(39) Ishida, T.; Cleri, F.; Kakushima, K.; Mita, M.; Sato, T.; Miyata, M.; Itamura, N.; Endo, J.; Toshiyoshi, H.; Sasaki, N.; Collard, D.; Fujita, H. *Nanotechnology* **2011**, *22*, 355704.

(40) Han, X.-L.; Larrieu, G.; Fazzini, P.-F.; Dubois, E. *Microelectronic Engineering* **2011**, *88*, 2622 – 2624.

(41) Baykan, M. O.; Thompson, S. E.; Nishida, T. *Journal of Applied Physics* **2010**, *108*, 093716.

(42) Xu, H.; Liu, X.; Du, G.; Fan, C.; Jin, R.; Han, R.; Kang, J. *Nanotechnology, IEEE Transactions on* **2011**, *10*, 1126 –1130.

TABLE

Table 1: Main physical mechanism governing the retarded or self-limited oxidation with decreasing convex or concave nanobjects size.

Character	σ_r	P	Origin
Convex	$\nearrow$	$\ll$	Limited reaction rate
Concave	$\ll$	$\nearrow$	Limited Diffusion mechanism

FIGURE CAPTIONS

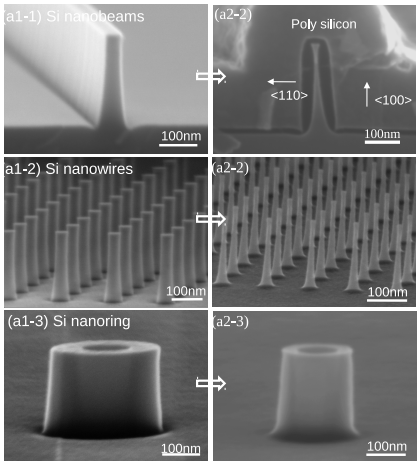

Figure 1: Serial a1 (1-3): SEM pictures of silicon nanostructures after fabrication; Serial a2 (1-3): SEM pictures after wet oxidation and oxide stripping

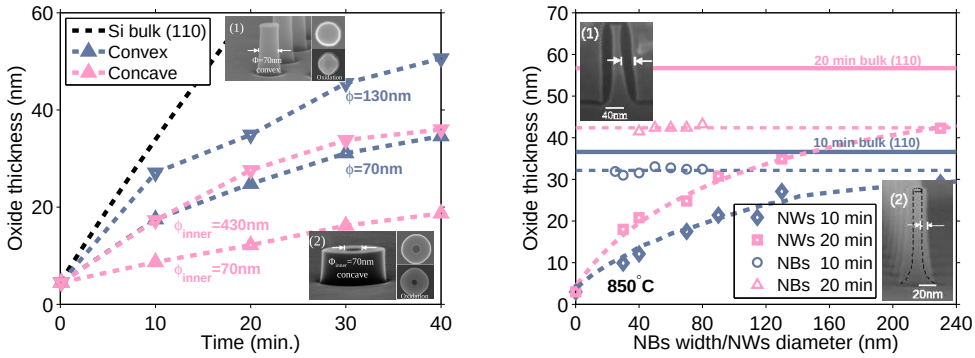

(a) (b)

Figure 2: (a) Convexity vs concavity: the various symbols present the experimental oxide thickness for SiNWs (convex nanostructure) with diameters 70 nm, 130 nm and silicon nanorings (concave nanostructure) with inner diameters of 70 nm and 430 nm as a function of the oxidation time (b) Comparison between the oxide thickness in the middle edge of the Si nanobeams and SiNWs for wet oxidation of 10 min and 20 min at 850°C. The experimental trend is described by the dashed lines. Inset SEM images: (1) the Si nanobeams (cross-section view), (2) SiNWs (titled view) after oxidation where the position set to measure the oxide thickness is reported.

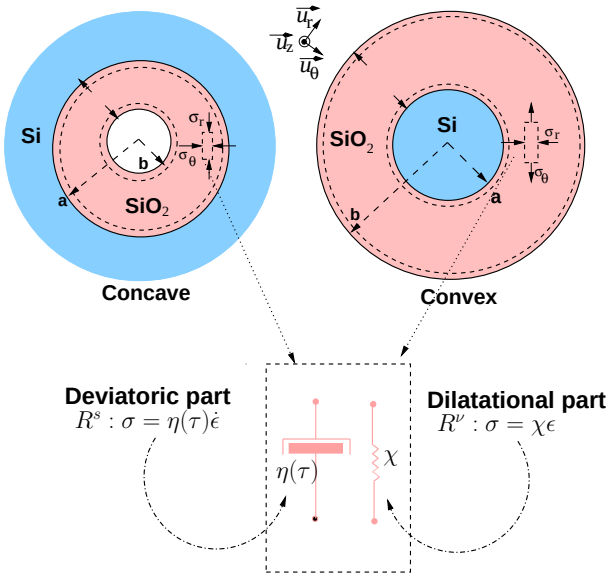

Figure 3: Schematics of the concave and convex cylinder nanostructure oxidation and resulting stress field in the silicon oxide. A compressive radial stress component is created in the two cases whereas the tangential component is initially compressive (resp. tensile) in the concave (resp. convex) case. The strain in the oxide could be divided into two components (the dilatational part) and the deviatoric part associated to shape modification. The dilatational part is often neglected compared to the deviatoric part for the SiO_2 mechanical behaviour and a dashpot is used for the stress/strain rate relationship; plasticity effects are introduced by considering a non-linear shear dependent viscosity $\eta(\tau)$.

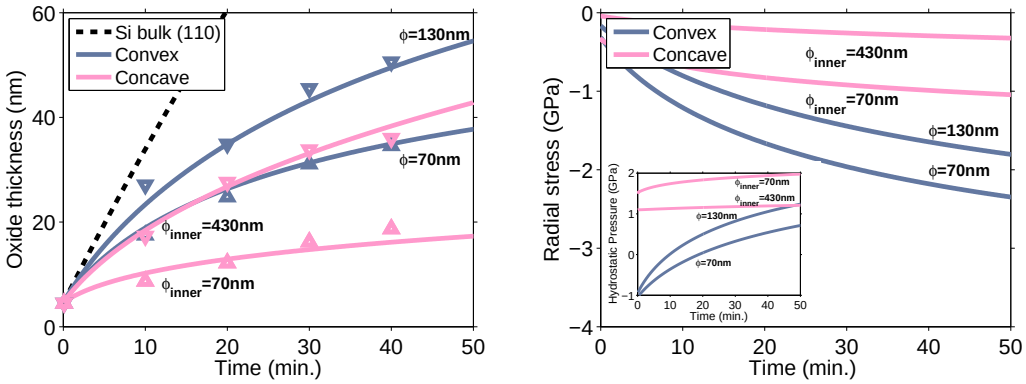

Figure 4: (a) Modelling of the convex/concave oxidation using the plastic model. b) Evolution of the theoretical radial stress σ_r at the Si/SiO_2 interface. Inset provides the hydrostatic pressure evolution during the oxidation for the different nanostructures.

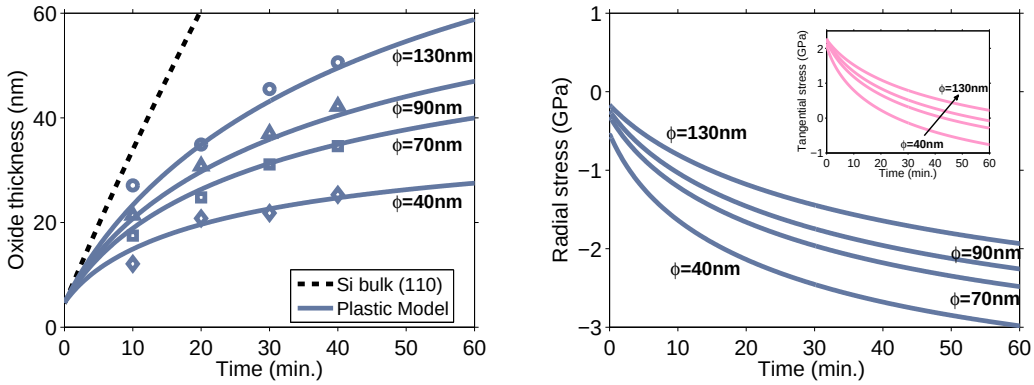

(a) (b)

Figure 5: (a) Experimental (symbols) and (continuous lines) oxidation kinetics dependence of SiNWs at 850°C as function of the SiNWs diameters and for various oxidation time. (b) reports the corresponding radial stress evolution. Inset (1) highlights the large tangential stress relaxation from 2 GPa down to zero or a slightly compressive stress of a hundreds MPa.

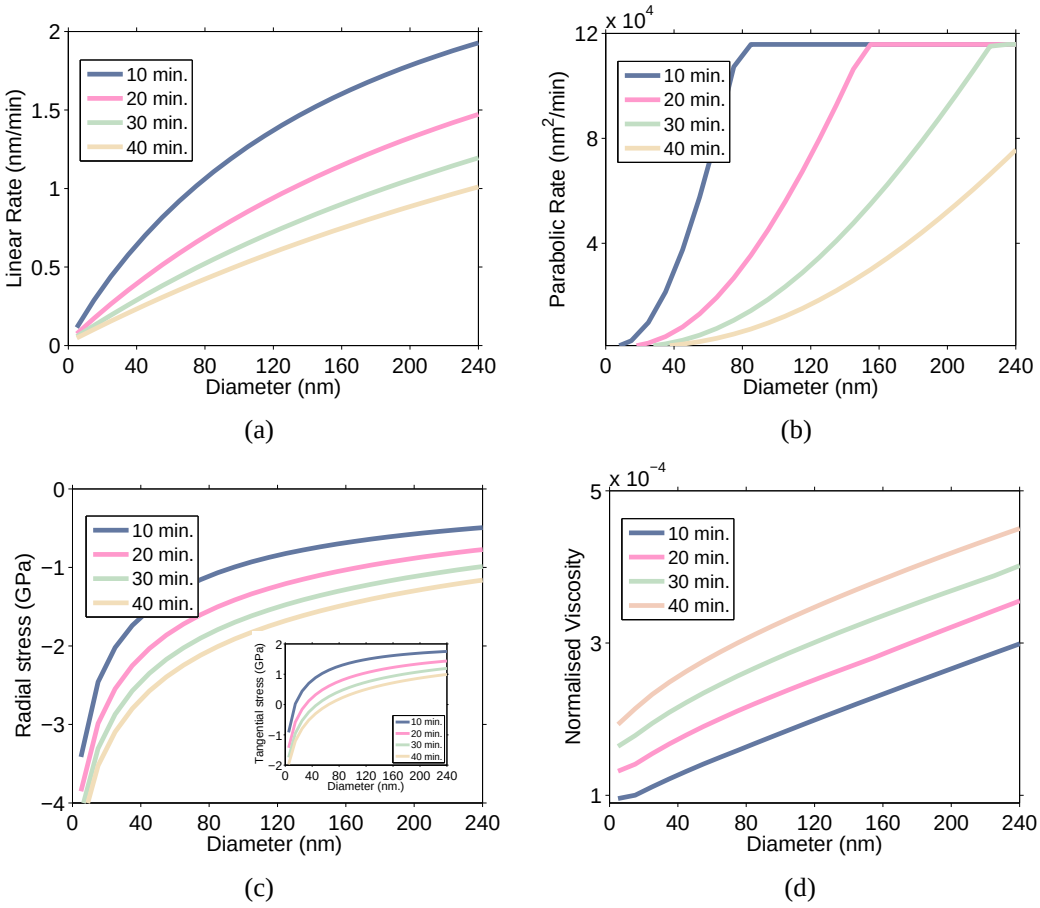

Figure 6: a) Linear rate variation with NWs diameters showing the impact of the radial stress in the initial oxidation regime as the main limiting factor. b) Highlight of the diffusion limited regime which takes place only when a sufficient oxide thickness has been grown. c) Illustration of the compressive radial stress build-up during oxidation with decreasing SiNWs diameters. Inset: tangential stress relaxation and transition from tensile to compressive with decreasing SiNW diameters. d) Impact on the normalised viscosity $\eta(\tau)/\eta_0$ strongly reduced by plasticity effects as the initial viscosity (η_0=1.4 10^{18} Poisse) is almost reduced by a factor 10^{04} with the shear stress influence $\eta(\tau)$.